Biosensors and Bioelectronics 26 (2011) 3142–3147

Contents lists available at ScienceDirect

Biosensors and Bioelectronics

journal homepage: www.elsevier.com/locate/bios

# Surface immobilization of DNA aptamers for biosensing and protein interaction analysis

Xiaojuan Zhang, Vamsi K. Yadavalli*

*Department of Chemical and Life Science Engineering, 601 W. Main Street, Virginia Commonwealth University, Richmond, VA 23284, United States*

ARTICLE INFO

*Article history:*
Received 3 September 2010
Received in revised form 6 November 2010
Accepted 8 December 2010
Available online 16 December 2010

*Keywords:*
QCM
Aptamer
Biosensor
AFM
Immunoglobulin E

ABSTRACT

To utilize aptamers as molecular recognition agents in biosensors and biodiagnostics, it is important to develop strategies for reliable immobilization of aptamers so that they retain their biophysical characteristics and binding abilities. Here we report on quartz crystal microbalance (QCM) measurements and atomic force microscope (AFM)-based force spectroscopy studies to evaluate aptasensors fabricated by different modification strategies. Gold surfaces were modified with mixed self assembled monolayers (SAMs) of aptamer and oligoethylene glycol (OEG) thiols ($HS\text{-}C_{11}\text{-}(EG)_nOH$, $n = 3$ *or* $6$) to impart resistance to nonspecific protein adsorption. By affinity analysis, we show that short OEG thiols have less impact on aptamer accessibility than longer chain thiols. Backfilling with OEG as a step subsequent to aptamer immobilization provides greater surface coverage than using aptamer and OEG thiol to form a mixed SAM in one-step. Immunoglobulin E and vascular endothelial growth factor (VEGF) were studied as target proteins in these experiments. Binding forces obtained by these strategies are similar, demonstrating that the biophysical properties of the aptamer on the sensors are independent from the immobilization strategy. The results present mixed SAMs with aptamers and co-adsorbents as a versatile strategy for aptamer sensor platforms including ultrasensitive biosensor design.



## 1. Introduction

Aptamers are synthetic, functional oligonucleotide receptors engineered with a high affinity and specificity towards diverse targets. By *in vitro* evolutionary selection – Systematic Evolution of Ligands by Exponential Enrichment (SELEX) (Ellington and Szostak, 1992), aptamers with distinguishing sequences and functional structures can be selected against a wide variety of targets including proteins, cells and small molecules (Bunka and Stockley, 2006). Compared to antibodies, aptamers have a comparable or greater affinity as capture molecules. Aptamers can be synthesized at low cost via *in vitro* procedures, and can be easily modified with different functional groups and tags, making them adaptable to various immobilization strategies for assay applications (Bunka and Stockley, 2006; Jayasena, 1999). Finally, we can regulate and manipulate the recognition process by rational design (Potty et al., 2009), with modifications for specific signal generation in a sensor format (Cho et al., 2009).

Several studies on aptamer-based biosensors have been reported, reflecting their enormous potential (Cho et al., 2009; Kirby et al., 2004; Navani and Li, 2006). Detection by aptamer-based sensors has been conducted by different methods, including Surface Plasmon Resonance (SPR), Quartz crystal microbalance (QCM), and fluorescence (Balamurugan et al., 2008; Hianik et al., 2005; Strehlitz et al., 2008). In particular, the label free QCM technique is a powerful tool in biological binding phenomena with advantages, including high sensitivity and real time measurement (Cooper and Singleton, 2007). The QCM has also been used as an active mode sensor for the direct detection of molecular interactions by oscillating the sensor surface and monitoring the acoustic emission produced by bond rupture (Dultsev et al., 2000).

To utilize an aptamer for biosensor applications, the first step of sensor design involves the immobilization of the aptamer to the sensor surface. Design challenges include minimization of nonspecific binding, loss of affinity and increasing the accessibility of the aptamer. There are several possible immobilization strategies for DNA based molecules (Beaucage, 2001). Anti-thrombin aptamers were modified with an amino group at the 3′ end, enabling covalent attachment to a glass surface via carbonylimidazole groups (Potyrailo et al., 1998) or aldehyde groups (Ho et al., 2009). Strategies for DNA immobilization in nucleic acid-based sensors with QCM detection of hybridization were developed several years ago in various formats including biotin attachment and direct adsorption (Caruso et al., 1997; Yamaguchi et al., 1993). These were adapted to aptamers in QCM biosensors with a biotin labeled anti-IgE aptamer immobilized on a streptavidin modified Au (Liss et al.,

* Corresponding author. Tel.: +1 804 828 0587; fax: +1 804 828 3846.
*E-mail address:* vyadavalli@vcu.edu (V.K. Yadavalli).

0956-5663/$ – see front matter © 2010 Elsevier B.V. All rights reserved.
doi:10.1016/j.bios.2010.12.012

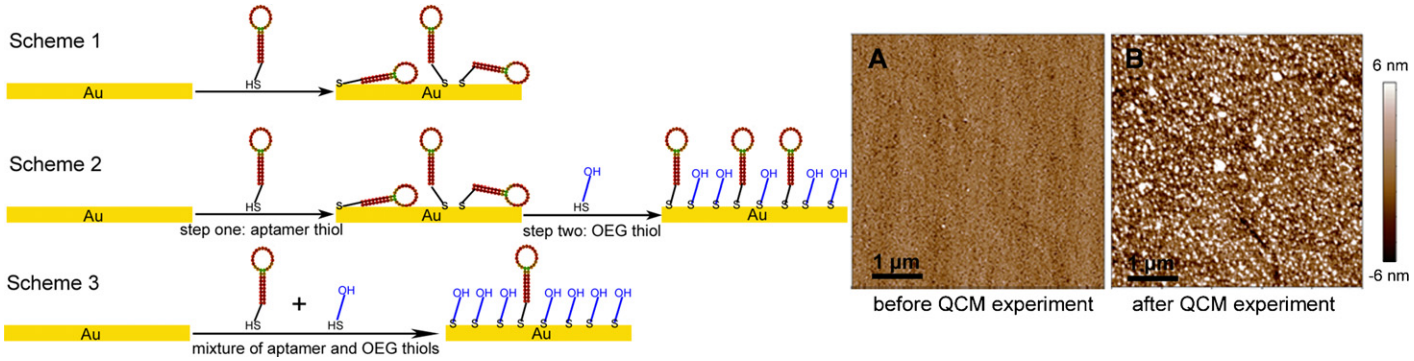


**Fig. 1.** (A) Schematic of different sensor configurations investigated. (B) and (C) AFM images of sensor surface modified by Scheme 2 (sensor B) before and after QCM experiments.

2002). Biotin/streptavidin immobilization strategies were also used in other aptamer biosensors (Hianik et al., 2005; Yao et al., 2010). However, the methods described take several steps to immobilize the aptamer, that can result in a higher risk for chemical contamination and loss of specificity of the sensor (Peterlinz et al., 1997). It is therefore vital to develop methods for the attachment of aptamers to surfaces for use in biosensors or diagnostics that involve minimal loss in functionality and non-specific interactions. Direct attachment of anti-thrombin aptamers to a gold surface was earlier demonstrated using alkane thiol linkers, with comparison of different co-adsorbent thiols of aptamers forming a mixed self assembled monolayer (SAM) (Balamurugan et al., 2006). SPR and ellipsometry were used to measure binding events. Current strategies in aptasensors design either involve synthesizing complex modular functional groups in the overall design of an aptamer or directly attaching them to a surface. The former strategy reduces simplicity and may also hinder the binding abilities of the selected aptamer. The latter strategy results in a large degree of non-specific adsorption of proteins to the sensor surface and also does not allow suitable control of surface distribution or orientation of aptamers. Optimizing the activity and accessibility of the aptamer for various biosensing applications still remains a key challenge.

Advantages to using a direct Au–S bond to attach a receptor molecule include a rapid, covalent reaction and formation of a stable monolayer. Thiol chemistry allows the selection of functional groups that may be used as co-adsorbents to form mixed SAMs with different surface properties (Ulman, 1996). Here we investigate three facile strategies (Fig. 1) for the direct attachment of aptamers to gold surfaces for biosensing and protein interaction analyses. The first is the direct formation of an aptamer SAM via thiol attachment to a gold surface. The second is a two-step mixed-SAM formation: aptamer SAM self-assembly, followed by backfilling of the unmodified surface with an oligoethylene glycol (OEG) thiol. The third involves the formation of a mixed-SAM in a single step via co-adsorption from a solution of a thiol-modified aptamer and OEG thiol. The aptamer is modified at the 5′-end with a $(CH_2)_6$ spacer and an –SH linker, for direct covalent immobilization to gold.

QCM measurements were conducted to evaluate the sensitivity and affinity of the aptamer sensors fabricated. The characterized immunoglobulin E (IgE) aptamer/IgE system was chosen as a model system to evaluate and optimize the methods in an initial set of experiments. This provides a basis to test both the biophysical and sensing abilities of our sensors. To further verify the functional viability of the surface-tethered aptamers for biophysical analyses and protein binding, atomic force microscopy (AFM) based force spectroscopy of the binding pairs was performed. A second system of the angiogenic protein vascular endothelial growth factor (VEGF) and the VEGF-binding aptamer were tested with the strategy evaluated. The comparison between these strategies is reported here along with correlation between affinities and rupture forces. These methods can be used to form active aptamer-surfaces for sensing applications and study fundamental molecular interactions between aptamers and their targets.

## 2. Experimental

### 2.1. Materials and instrumentation

IgE binding DNA aptamer (anti-IgE) (5′-GGG GCA CGT TTATCC GTC CCT CCT AGT GGC GTG CCC C-3′), and $VEGF_{165}$ binding DNA aptamer (anti-VEGF) (5′-CCGTCTTCCAGACAAGAGTGCAGGG-3′) with 5′ dithiol S–S modifiers and $(CH_2)_6$ spacers were custom synthesized by Integrated DNA Technologies, Inc. (Coralville, IA). Anti-Human IgE produced in goat was purchased from Sigma Aldrich, and recombinant $VEGF_{165}$ was obtained from Biovision, Inc. (Mountain view, CA).

(1-Mercaptoundec-11-yl) hexaethylene glycol (HS-$C_{11}$-$(EG)_6$ OH) (1-mercaptoundec-11-yl) triethylene glycol (HS-$C_{11}$-$(EG)_3$OH) and (1-mercaptohexadecanoic acid)-N-succinimidyl ester (NHS-terminated thiol), HS-$C_{15}$-COO-NHS, were purchased from Nanoscience Instruments (Phoenix, AZ). We refer to HS-$C_{11}$-$(EG)_6$OH and HS-$C_{11}$-$(EG)_3$OH thiols as $EG_6$ and $EG_3$ respectively. Phosphate-buffered saline (PBS pH 7.4) (11.9 mM phosphates, 137 mM sodium chloride and 2.7 mM potassium chloride), 1 M $MgCl_2$ solution (molecular biology grade) and Ethanol (200-proof) were purchased from Fisher Scientific. DEPC treated RNase free water was used for all experiments.

QCM measurements were performed using a Q-Sense E4 system (Q-Sense AB, Gothenburg, Sweden). Gold coated QCM crystal sensors (QSX 301) were purchased from QSense. Gold surfaces were purchased from Agilent Technologies, Inc. (Foster City, CA).

### 2.2. Functionalized sensor,substrate and probe preparation

Gold sensors and substrates were cleaned by UV/ozone treatment for 10 min, rinsing with ethanol and RNase free water, followed by UV/ozone treatment for 10 min. The resulting clean surfaces were modified by different strategies (Fig. 1). Scheme 1: immersion in 2.5 μM solution of a thiolated aptamer (HS-$C_6$-aptamer) in RNase free water overnight (16 h), and rinsing with RNase free water; Scheme 2: two-step mixed monolayer modification: immersion in a thiolated aptamer (HS-$C_6$-aptamer) water solution for 2 h, followed by rinsing with water. Subsequent immersion in either HS-$C_{11}$-$(EG)_3$OH or HS-$C_{11}$-$(EG)_6$OH ethanol solution overnight (16 h), and rinsing with ethanol. Scheme 3: one-step mixed monolayer modification: immersion in a water solution containing both thiolated aptamer (HS-$C_6$-aptamer) and HS-$C_{11}$-$(EG)_3$OH overnight (16 h), then rinsing with

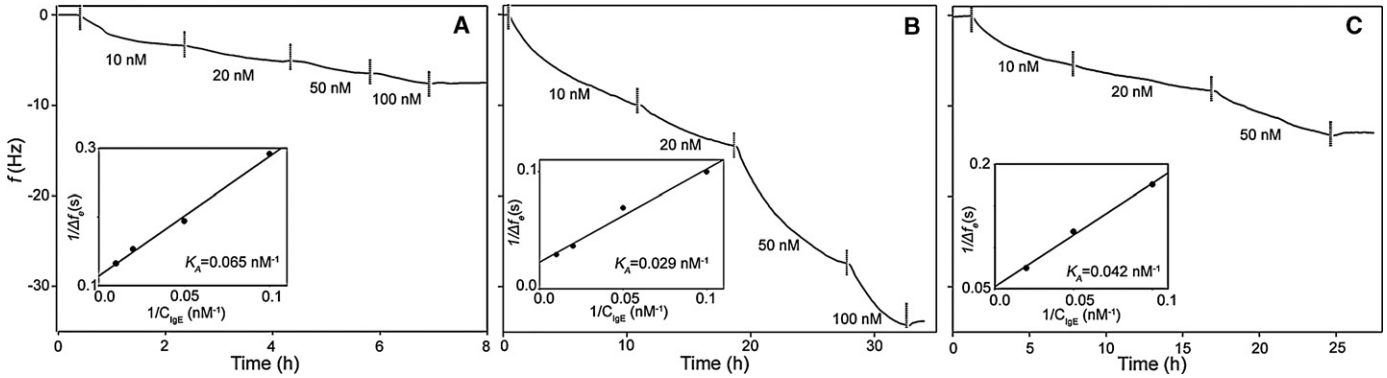


**Fig. 2.** QCM frequency response to IgE: sensor A: two-step modification, aptamer 0.25 μM, $EG_6$ 1 mM; sensor B: two-step modification, aptamer 0.25 μM, $EG_3$ 1 mM; sensor C: one-step modification, 25 μM, $EG_3$ 1 mM; Insets – $K_A$ estimated from $1/\Delta f_e$ as a function of $1/C_{IgE}$ for each sensor.

water. Sensors were fabricated under similar conditions to ensure consistency with respect to immobilization time and monolayer formation.

Gold coated AFM cantilevers were UV/ozone cleaned for 10 min. Cantilevers were functionalized by self-assembled monolayers prepared as described (Yadavalli et al., 2006) – immersion in mixed thiol solution (HS-$C_{11}$-$(EG)_6$OH and HS-$C_{15}$COO-NHS) in ethanol for 16 h. Surfaces were then rinsed with ethanol, and incubated in a 100 nM solution of protein (IgE or VEGF) in PBS buffer for 1 h at room temperature.

### 2.3. Quartz crystal microbalance measurements

The QCM sensors used are 14 mm diameter discs, optically polished AT-cut quartz crystals with Au coating (10 mm diameter) on both sides. Sensors operate at a fundamental frequency of 4.95 ($f_0$) MHz. Frequency at multiple overtones was measured simultaneously. In this study, the results shown are the normalized frequencies calculated from third overtone ($f_3/3$). Before each measurement, buffer was passed through the QCM flow module for 2–4 h to obtain a stable baseline. All measurements were carried out under constant flow rates of 8.6 μl/min, and at 20 °C.

### 2.4. AFM imaging of surfaces and force spectroscopy

Gold coated PPP-CONTCSAu cantilevers from Nanosensors (Neuchatel, Switzerland), TR400 PB and TR800PSA cantilevers from Olympus (Tokyo, Japan) were used for force measurement and imaging respectively. AFM imaging and force spectroscopy experiments were performed using an Asylum MFP-3D atomic force microscope (Asylum Research, Santa Barbara, CA). TR800PSA cantilevers ($k \sim 0.15$ N/m, frequency 24 kHz) was used for imaging the surfaces in noncontact (tapping) mode. TR400 PB cantilevers ($k \sim 0.09$ N/m, frequency 24 kHz) functionalized with the aptamer as described, were used for measurement of interaction forces. Regions with protein molecules were identified prior to force spectroscopy by non-contact imaging. Force-distance curves were obtained by moving the tip to these locations, holding in place for 5 s to allow binding and retracted. The force of contact was kept <300 pN to avoid damaging the functionalized AFM tip and surface. Force curves that showed rupture events at rupture lengths between 10 and 80 nm were selected and analyzed in IgorPro (Wavemetrics, OR) to determine the rupture force distributions. The $\chi^2$ statistic was used as a measure of the goodness of fit. Binding probability was estimated as the percentage of analyzed curves to the total number of curves collected in each experiment.

## 3. Results and discussion

### 3.1. IgE binding to thiolated anti-IgE aptamer monolayer

The resonance frequency of the quartz crystal sensor changes due to changes of its mass load. From the Sauerbrey equation, the change of frequency, $\Delta f$, is linearly correlated to its mass change, $\Delta m$

$$\Delta f = -56.5 \times 10^{-3} \frac{\Delta m}{A} \quad (1)$$

where $A$ ($cm^2$) is the surface area of the sensor, $\Delta f$ and $\Delta m$ are in Hz and ng respectively. In our experiments, $A = 78.5 \times 10^{-2}$ $cm^2$, $f_0$ (the fundamental frequency of crystal) = 4.95 MHz (manufacturer supplied), implying that 1 μg mass load would cause a ~72 Hz frequency change. The sensitivity constant in Eq. (1) ($ng^{-1}$ $cm^2$ Hz) has been obtained assuming a value of the quartz density (2648 kg $m^{-3}$); and the velocity of sound in the quartz crystal (3340 m $s^{-1}$) at room temperature (Liss et al., 2002).

In the initial set of experiments, we studied the binding of IgE to a sensor with pure anti-IgE aptamers immobilized on the surface. Different concentrations of the protein (IgE) were flowed over the sensor and the value of the steady-state frequency was used to estimate the corresponding binding affinity of IgE. In all experiments, we define a steady-state when the frequency change of the signal is <0.5 Hz/h. Based on the frequency response at different IgE concentrations, the binding affinity between two biomolecules at equilibrium, $K_A$ was estimated. The relationship between frequency changes and the affinity constant was derived (Liu et al., 2003):

$$\frac{1}{\Delta f_e} = \frac{1}{\Delta f_{max}} + \frac{1}{\Delta f_{max} K_A C_{IgE}} \quad (2)$$

where $C_{IgE}$ is the concentration of the protein, $\Delta f_e$ is the frequency change of crystal sensor after it reaches equilibrium, and $\Delta f_{max}$ represents the maximum frequency drop, which is an ideal state in which all accessible aptamers are bound to the target. From Eq. (2), the plot of $1/\Delta f_e$ as a function of $1/C_{IgE}$ is a straight line, and the affinity constant $K_A$ is determined as the quotient of the intercept and the slope. This linear relationship between $1/\Delta f_e$ and $1/C_{IgE}$ is supported by our observation resulting in a $K_A = 0.64$ $nM^{-1}$ for this system (Supplemental information Fig. S1).

The dissociation constant $K_D$ for this aptamer and IgE was measured as 10 nM through nitrocellulose filter partitioning analysis (Wiegand et al., 1996) and 8.4 nM via QCM measurement in an earlier study (Liss et al., 2002). $K_A$ can be calculated from these $K_D$ values as 0.10 $nM^{-1}$ and 0.12 $nM^{-1}$ respectively. Compared to these reported values, this sensor shows a higher binding affinity, while maintaining a low detection limit <10 nM.

However, this immobilization strategy with direct attachment of thiolated DNA SAMs on gold was earlier shown by hybridization studies to be non-optimal (Balamurugan et al., 2006; Herne and Tarlov, 1997). First, interactions between Au surface and DNA are not exclusively through thiol groups modified at the 5′-end, but also through nitrogen moieties within the nucleotide bases. The DNA therefore, tends to nonspecifically bind to the gold surface, resulting in reduced accessibility of the aptamer and a disordered orientation. Second, the repulsion between DNA chains may result in poorer surface coverage, especially at low ionic strength buffer conditions (Balamurugan et al., 2006; Herne and Tarlov, 1997). The resulting uneven coverage results in nonspecific adsorption of analytes to the bare Au surface. It can therefore be expected that, for aptamer-based protein sensors, both the nonspecific adsorption and reduced accessibility can affect its function, and cause inaccuracy of measurement. To minimize these effects, we used a mixed SAM strategy of thiolated aptamers with passivating thiols as co-adsorbents to fabricate stable, specific aptasensors.

### 3.2. IgE binding to mixed self-assembled monolayers

To form mixed aptamer SAMs, a co-adsorbent thiol can be used to fill the Au surface between the DNA molecules and thereby reduce nonspecific interactions between Au and DNA (Boozer et al., 2006; Herne and Tarlov, 1997). Here, we utilize oligo-ethylene glycol (OEG) thiols as co-adsorbents with thiol-modified aptamers to form mixed SAMs for QCM based aptasensors. SAMs of OEG-terminated thiols have been well documented as effective protein-resistant monolayers, with $EG_3$ and $EG_6$ being most widely used (Li et al., 2005; Prime and Whitesides, 1993).

Two different strategies to form mixed SAMs were studied: (1) A two-step method where the aptamer thiol was first immobilized on a gold surface, followed by backfilling of the bare gold area with an OEG thiol (Fig. 1 and Scheme 2 – sensors A and B – backfilling with $EG_6$ and $EG_3$ respectively). This strategy can enhance the utilization of the aptamer and minimize possible contamination caused by the mixing process. (2) A single step method using a mixture of the aptamer-thiol and OEG-thiol in water (Fig. 1 and Scheme 3 – sensor C) to form the SAM. Previous studies have shown that water is also a suitable solvent for the formation of ordered mixed SAMs of ssDNA and OEG on Au surface (Boozer et al., 2006). This strategy allows control of the aptamer coverage on the surface by simply changing the molar ratio of the two thiols in solution. Control sensors (containing no sensing aptamer) modified by $EG_3$ or $EG_6$ alone were used to determine the extent of non-specific adsorption to the sensor surfaces.

Typical QCM curves obtained are shown in Fig. 2. Binding affinities were analyzed based on the changes in frequency observed (Fig. 2 insets). $K_A$ values for sensors A, B and C are calculated as $0.058 \pm 0.009\ nM^{-1}$, $0.030 \pm 0.002\ nM^{-1}$ and $0.041 \pm 0.003\ nM^{-1}$ respectively. Compared to the $K_A$ values analyzed by the sensor modified by aptamer thiol alone (Scheme 1), these results are consistent with that measured by previous studies ($K_A = 0.10\ nM^{-1}$). Sensor A shows the highest IgE affinity but a low frequency response at each IgE concentration. Sensors B and C were modified with mixed SAMs of aptamer and $EG_3$, by Schemes 2 and 3 respectively. While the $K_A$ values are similar, sensor C shows a reduced frequency response at each IgE concentration, although the concentration of aptamer in the thiol solution is 100 times the aptamer concentration for sensor B. In all sensors, low concentrations <10 nM of the IgE can be reliably detected, showing that this strategy is useful to create sensitive sensors with reduced non-specificity. Fig. 1B and C show AFM images of sensors before and after QCM experiments respectively. Fig. 1C shows coverage of the surface with IgE, bound to the immobilized aptamer.

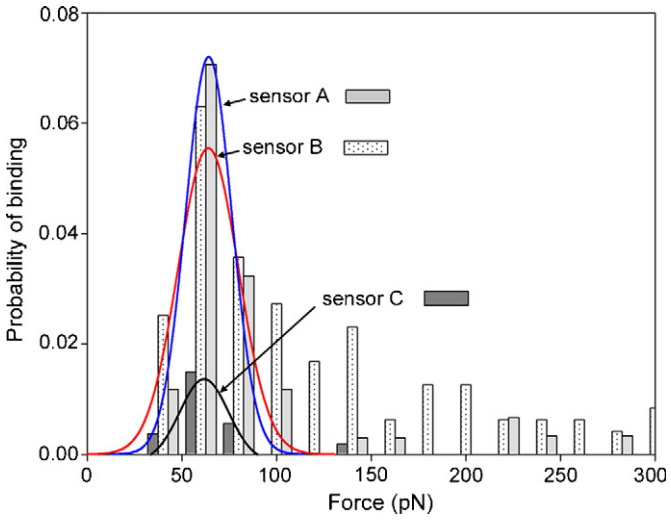


**Fig. 3.** Force distribution of IgE immobilized AFM tip towards different mixed SAM surfaces. Gaussians represent force peaks of $64.1 \pm 0.9$ pN, $64.0 \pm 2.9$ pN and $61.7 \pm 0.7$ pN for sensors A, B and C respectively.

The frequency drop of the sensors was calculated at equilibrium at a flow of 20 nM IgE where the frequency drop is directly correlated to the amount of bound protein. As expected, sensors modified by OEG thiol alone, have a much smaller frequency drop compared with those modified with aptamer thiol SAMs. While longer chain $EG_6$ has been shown to exhibit a better resistance to protein adsorption than $EG_3$ (Prime and Whitesides, 1993), in our experiments, the sensor A with immobilized aptamer thiol and $EG_6$ thiol does not show significant response compared with $EG_6$ thiol alone. With the $EG_3$ thiol as co-adsorbent, the sensor modified by the aptamer and $EG_3$ thiol (sensor B) has a significantly increased response towards IgE (Supplementary Information Fig. S2). This is likely because the aptamer surrounded by the longer chain $EG_6$ may result in poorer accessibility of the aptamer. On the contrary, the shorter chain $EG_3$ thiol has considerably less impact on the accessibility of aptamer, making it a better choice for sensor fabrication.

### 3.3. AFM force spectroscopy of IgE/anti-IgE aptamer system on mixed SAMs

By QCM measurements, different mixed SAM strategies display ability to resist nonspecific adsorption, and show a better binding to IgE than the aptamer alone. However, sensors functionalized in different conditions showed different affinity towards IgE (Fig. 2). One underlying reason for this could be due to the difference of biological activity of aptamer caused by different immobilization strategies. Another possibility is due to the differences in accessibility of aptamer caused by different length of OEG thiol, or surface thiol coverage.

To further explain the different affinities, molecular force spectroscopy using atomic force microscopy was applied to study the rupture forces between IgE and the immobilized aptamer in each sensor. The AFM is a powerful analytical tool that has been used to study a variety of biomolecular interactions at the molecular level (Hinterdorfer and Dufrene, 2006). The biophysical differences of aptamer immobilized by different strategies can be observed through force spectroscopy study. In addition, the AFM as a molecular recognition force probe forms a viable tool for the ultrasensitive detection of analytes using aptamers.

Rupture forces were measured and analyzed on surfaces modified, corresponding to the sensors A, B and C, respectively. As shown in Fig. 3, similar rupture force distributions were obtained from

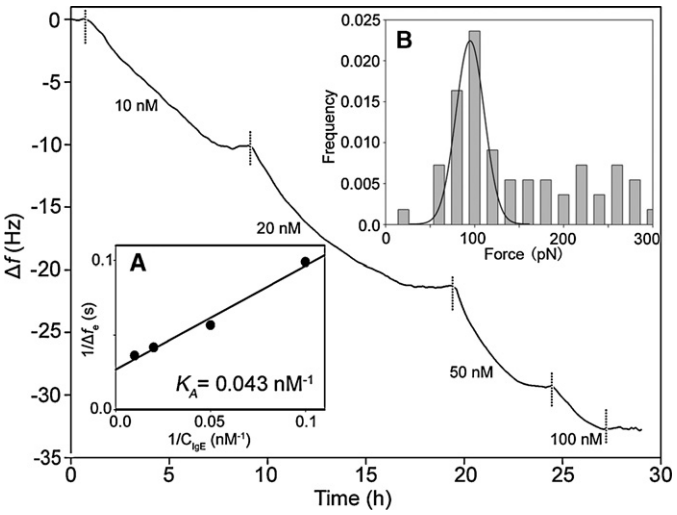


**Fig. 4.** QCM frequency response of sensor to varying concentrations of VEGF. Inset A – $K_A$ estimated from $1/\Delta f_e$ as a function of $1/C_{IgE}$; Inset B – AFM rupture force distribution of VEGF and anti-VEGF aptamer on Sensor B for IgE/anti-IgE system.

all three sensors, at 64.1 ± 0.9 pN, 64.0 ± 2.9 pN and 61.7 ± 0.7 pN (Table 1). However, the frequency of binding events is different, especially for Scheme 3 (sensor C) where the percentage of total binding events is 3.2%, which is much lower than 27.5% (sensor B) and 16.7% (sensor A) for two-step modification strategies. This result is consistent with the low frequency response of QCM sensors modified by an identical strategy. It appears that in the presence of a mixture of OEG and aptamer thiol, the surface coverage of the aptamer is significantly lower. For two-step modifications, aptamer/$EG_3$ surface (sensor B) has a higher percentage of total binding events compared to aptamer/$EG_6$ (sensor A). This may be explained by the better accessibility of aptamer towards IgE because of the shorter chain of $EG_3$ compared with $EG_6$.

### 3.4. VEGF binding to mixed SAMs of thiolated anti-VEGF aptamer and OEG thiol

Finally, the efficacy of the mixed aptamer thiol strategy was tested using a different protein/aptamer system. The aptamer for the angiogenic protein vascular endothelial growth factor (VEGF) (Potty et al., 2009) was investigated via QCM and AFM. QCM measurement was conducted with the sensor modified with anti-VEGF aptamer and $EG_3$ thiol by incubating with 0.25 μM aptamer followed by 1 mM $EG_3$ (Scheme 2). The rupture force between the aptamer and target (VEGF) was measured on the same surface using a VEGF functionalized AFM cantilever (Fig. 4, inset B). From the frequency response of the QCM experiment (Fig. 4), the $K_A$ = 0.043 nM$^{-1}$. This value is higher than the $K_A$ of 0.029 nM$^{-1}$ for the IgE aptamer/IgE system by the same modification. The $K_A$ is close to the reported value of the affinity constant (0.092 nM$^{-1}$) obtained earlier for the DNA aptamer using SPR (Potty et al., 2009). It may be noted that the increased affinity of the VEGF pair is also accompanied by a much higher rupture force (95.0 ± 2.5 pN) for this system, which is much higher than the value of IgE/anti-IgE aptamer system.

### 3.5. Aptamer surface density, accessibility and affinity towards its target

The rupture forces from all surfaces are consistent at 60–65 pN. This implies that, at the molecular level, the immobilized aptamers retain similar biophysical characteristics and structure, although attached via different strategies. We hypothesize that different affinity values from QCM experiments are likely caused by the interactions and aptamer accessibility due to the surrounding OEG thiols. The length, the density and the regularity of the OEG thiol coverage depends on the type of thiols and also on the immobilization process. These factors determine the ability of the surface to resist nonspecific adsorption of IgE and affect the accessibility of the aptamer towards its target. It has also been demonstrated earlier that OEG thiols have the ability to stabilize and control the orientation of DNA on a surface (Boozer et al., 2006), further increasing the utility of this strategy.

The theoretical thickness of monolayers formed by $EG_3$ and $EG_6$ thiols are 22.4 Å and 30.8 Å respectively (Harder et al., 1998). The co-adsorbent thiol can reduce the nonspecific adhesion between DNA and gold surface, while improving the orientation of aptamer. Compared to the $EG_6$ thiol, the $EG_3$ thiol is shorter, allowing most of the stem structure to be exposed resulting in a better binding to the protein target.

Although the 1:40 molar ratio of aptamer:OEG used to prepare sensor C is 100 times higher than that used in sensor B, the total binding was estimated to be 80.9 ng, which is 56% of that in sensor B. This implies that the surface coverage of the aptamer immobilized in this one-step modification procedure is dilute compared to sensor B. The calculated $K_A$ of the aptamers by these two methods are almost similar, although sensor C shows a slightly higher affinity than sensor B. This difference is likely due to better separation of the aptamer on the surface, resulting in easier adaptive binding towards its target. Suitable optimization of the molar ratios of the aptamer and OEG can therefore be used to increase both the binding and affinity of the immobilized aptamer.

As measured earlier, the unbinding/rupture force for an antigen/antibody pair can be determined from the free enthalpy $\Delta H$ and the effective range of the potential $d$, given by $F = \Delta H/d$. For a $K_A$ between $10^2$ and $10^{10}$ M$^{-1}$, the rupture force is therefore estimated to be between 35 and 165 pN (Dammer et al., 1996). In these experiments, the $K_A \sim 3 \times 10^7$ M$^{-1}$, and rupture force ~65 pN for the IgE system and $4 \times 10^7$ M$^{-1}$, and rupture force ~95 pN for the VEGF system, showing that the aptamer/protein pairs behave in a similar and consistent fashion. This was consistent to that observed earlier by force spectroscopy of the IgE aptamer/IgE (Jiang et al., 2003).

The key advance in this paper is to demonstrate facile immobilization strategies for aptamers for use in a variety of different biosensors. Aptasensors fabricated by these strategies have low nanomolar detection limits of different analytes. We show that the biophysical characteristics of the aptamer at the molecular remain undisturbed regardless of immobilization strategy. However, sensor accessibility is affected by the choice of the surrounding functional groups as manifested by a decreased probability of binding. This molecular level information has a direct effect on key biosensor parameters including specificity, limits of detection and reduction of non-specific adsorption to the sensor surface as shown using QCM, which are the measurements of the ensemble aver-

**Table 1**
Comparison of affinity and rupture force for each sensor. The $K_A$ value is obtained from QCM measurements; and the rupture force from AFM measurements.

| Sensor | Modification | Aptamer conc. | OEG | $K_A$ (nM$^{-1}$) | Rupture force (pN) |
|---|---|---|---|---|---|
| A | Two-step | 0.25 μM | $EG_6$ | 0.058 ± 0.009 | 64.1 ± 0.9 |
| B | Two-step | 0.25 μM | $EG_3$ | 0.030 ± 0.002 | 64.0 ± 2.9 |
| C | One-step | 25 μM | $EG_3$ | 0.041 ± 0.003 | 61.7 ± 0.7 |

age of thousands of aptamer molecules. To our knowledge, this the first study that investigates aptamer parameters across different length scales – molecular to the ensemble (bulk) scale. The additional advantage of the strategies demonstrated is to provide a platform to conduct fundamental biophysical studies on aptamers including understanding their rupture forces and conformational changes at the molecular level. The interplay of aptamer specificity, selectivity and conformational rigidity at the molecular level have important roles in determining how aptamers bind their specific targets (Zhang and Yadavalli, 2010). The platforms demonstrated in this study can further be used for useful molecular investigations of different systems. Aptamer selection via molecular design can thereby enable rational design of aptamer-based biosensors and biodiagnostic devices to optimize ensemble state sensing schemes.

## 4. Conclusion

Different modification strategies for immobilizing thiol-modified aptamers directly on Au surfaces were studied using QCM and AFM force spectroscopy, translating information across different length scales. Mixed SAMs with aptamer and OEG thiols as co-adsorbents showed a resistance to nonspecific protein adsorption, improved the sensing performance of sensor and were verified as a versatile platform for biophysical analyses. Sensors had high sensitivity and dynamic range with higher specificity. While the $EG_6$ thiol has better resistance to nonspecific protein adsorption compared to the $EG_3$ thiol, it results in reduced accessibility of the aptamer. In the different systems, similar rupture forces were required to unbind aptamer and protein and the relationship between the force and the affinity constant were consistent with energy calculations shown for antigen–antibody binding. By judicious choice of end groups and chain lengths, we can impart multiple functionalities on the same surface as the aptamer sensing element. This study demonstrates simple and versatile strategies that can be used both as aptamer sensor platforms for ultrasensitive analyte detection with minimal non-specific binding as well as for molecular and biophysical studies of aptamer–protein interactions.

## Acknowledgements

This research was partially supported by a grant (J-922) from the Thomas F. and Kate Miller Jeffress Memorial Trust. Dr. Kenneth J. Wynne is acknowledged for kind access to the QCM.

## Appendix A. Supplementary data

Supplementary data associated with this article can be found, in the online version, at doi:10.1016/j.bios.2010.12.012.

## References

Balamurugan, S., Obubuafo, A., Soper, S.A., McCarley, R.L., Spivak, D.A., 2006. Langmuir 22 (14), 6446–6453.
Balamurugan, S., Obubuafo, A., Soper, S.A., Spivak, D.A., 2008. Anal. Bioanal. Chem. 390 (4), 1009–1021.
Beaucage, S.L., 2001. Curr. Med. Chem. 8 (10), 1213–1244.
Boozer, C., Chen, S.F., Jiang, S.Y., 2006. Langmuir 22 (10), 4694–4698.
Bunka, D.H.J., Stockley, P.G., 2006. Nat. Rev. Microbiol. 4 (8), 588–596.
Caruso, F., Rodda, E., Furlong, D.F., Niikura, K., Okahata, Y., 1997. Anal. Chem. 69 (11), 2043–2049.
Cho, E.J., Lee, J.-W., Ellington, A.D., 2009. Annu. Rev. Anal. Chem. 2 (12), 12.11–12.24.
Cooper, M.A., Singleton, V.T., 2007. J. Mol. Recognit. 20 (3), 154–184.
Dammer, U., Hegner, M., Anselmetti, D., Wagner, P., Dreier, M., Huber, W., Guntherodt, H.J., 1996. Biophys. J. 70 (5), 2437–2441.
Dultsev, F.N., Ostanin, V.P., Klenerman, D., 2000. Langmuir 16 (11), 5036–5040.
Ellington, A.D., Szostak, J.W., 1992. Nature 355 (6363), 850–852.
Harder, P., Grunze, M., Dahint, R., Whitesides, G.M., Laibinis, P.E., 1998. J. Phys. Chem. B 102 (2), 426–436.
Herne, T.M., Tarlov, M.J., 1997. J. Am. Chem. Soc. 119 (38), 8916–8920.
Hianik, T., Ostatna, V., Zajacova, Z., Stoikova, E., Evtugyn, G., 2005. Bioorg. Med. Chem. Lett. 15 (2), 291–295.
Hinterdorfer, P., Dufrene, Y.F., 2006. Nat. Methods 3 (5), 347–355.
Ho, D., Falter, K., Severin, P., Gaub, H.E., 2009. Anal. Chem. 81 (8), 3159–3164.
Jayasena, S.D., 1999. Clin. Chem. 45 (9), 1628–1650.
Jiang, Y.X., Zhu, C.F., Ling, L.S., Wan, L.J., Fang, X.H., Bai, C., 2003. Anal. Chem. 75 (9), 2112–2116.
Kirby, R., Cho, E.J., Gehrke, B., Bayer, T., Park, Y.S., Neikirk, D.P., McDevitt, J.T., Ellington, A.D., 2004. Anal. Chem. 76 (14), 4066–4075.
Li, L., Chen, S., Zheng, J., Ratner, B.D., Jiang, S., 2005. J. Phys. Chem. B 109, 2934–2941.
Liss, M., Petersen, B., Wolf, H., Prohaska, E., 2002. Anal. Chem. 74 (17), 4488–4495.
Liu, Y., Yu, X., Zhao, R., Shangguan, D.H., Bo, Z.Y., Liu, G.Q., 2003. Biosens. Bioelectron. 19 (1), 9–19.
Navani, N.K., Li, Y.F., 2006. Curr. Opin. Chem. Biol. 10 (3), 272–281.
Peterlinz, K.A., Georgiadis, R.M., Herne, T.M., Tarlov, M.J., 1997. J. Am. Chem. Soc. 119 (14), 3401–3402.
Potty, A.S.R., Kourentzi, K., Fang, H., Jackson, G.W., Zhang, X., Legge, G.B., Willson, R.C., 2009. Biopolymers 91 (2), 145–156.
Potyrailo, R.A., Conrad, R.C., Ellington, A.D., Hieftje, G.M., 1998. Anal. Chem. 70 (16), 3419–3425.
Prime, K.L., Whitesides, G.M., 1993. J. Am. Chem. Soc. 115, 10714–10721.
Strehlitz, B., Nikolaus, N., Stoltenburg, R., 2008. Sensors 8 (7), 4296–4307.
Ulman, A., 1996. Chem. Rev. 96 (4), 1533–1554.
Wiegand, T.W., Williams, P.B., Dreskin, S.C., Jouvin, M.H., Kinet, J.P., Tasset, D., 1996. J. Immunol. 157 (1), 221–230.
Yadavalli, V.K., Forbes, J.G., Wang, K., 2006. Langmuir 22 (16), 6969–6976.
Yamaguchi, S., Shimomura, T., Tatsuma, T., Oyama, N., 1993. Anal. Chem. 65 (14), 1925–1927.
Yao, C.Y., Zhu, T.Y., Qi, Y.Z., Zhao, Y.H., Xia, H., Fu, W.L., 2010. Sensors 10 (6), 5859–5871.
Zhang, X., Yadavalli, V.K., 2010. Analyst 135, 2014–2021.